# Temperature Dependent Characteristics of Activated Carbons from Walnut Shells for Improved Supercapacitor Performance

**V.V. Pavlenko[1,2,3*], Q. Abbas[1], P. Przygocki[1], T. Kon'kova[4], Zh. Supiyeva[2], N. Abeykoon[5], N. Prikhodko[3,6], M. Bijsenbayev[3], A. Kurbatov[2], B.T. Lesbayev[2,3], Z.A. Mansurov[3]**

[1]Poznan University of Technology, Berdychowo 4, 60-965 Poznan, Poland
[2]Al-Farabi Kazakh National University, 71 al-Farabi Ave., 050040 Almaty, Kazakhstan
[3]Institute of Combustion Problems, Bogenbay Batyr str. 172, 050012 Almaty, Kazakhstan
[4]D. Mendeleev University of Chemical Technology of Russia, Miusskaya sq., 9, 125047 Moscow, Russia
[5]University of Texas at Dallas, 800 W Campbell Rd, 75080-3021 Richardson, USA
[6]Almaty University of Energetics and Communications, 126, Baytursinova St., 050013, Almaty, Kazakhstan

## Article info

## Abstract

Activated carbons (ACs) have been prepared from chemical treatment of walnut shells (WS) precursor at various temperatures (400–800 °C) by using phosphoric acid ($H_3PO_4$) as activating agent. Influence of activation temperature on the porosity development and capacitive properties of resulting carbons was investigated. Thermal post-treatment of carbons previously activated at moderate temperature, e.g. 400 °C allowed further structural and porosity modification. Then, these carbons were investigated by scanning electron microscopy, Raman spectroscopy, energy-dispersive X-ray spectroscopy, electrochemical techniques and low temperature nitrogen adsorption exhibiting high BET specific surface area of approximately 2100 $m^2$ $g^{-1}$ and a total pore volume up to 1.3 $cm^3$ $g^{-1}$. Carbon material obtained through activation by $H_3PO_4$ at 400 °C and post-treated at 800 °C was used to make electrodes which were implemented to realize AC/AC capacitor using 1 mol $L^{-1}$ $Li_2SO_4$. The electrochemical capacitor demonstrated high capacitance of 123 F $g^{-1}$ per mass of one electrode, reduced cell resistance and stable capacitance for 5000 galvanostatic charge/discharge cycles at 1.0 A $g^{-1}$.

## 1. Introduction

Activated carbons (ACs) are produced in large quantities every year owing to their increased demand in environmental and energy sectors. ACs are the material of choice in the field of energy storage e.g., as electrode materials for charge storage in supercapacitors (SCs) due to high conductivity and reduced cost of large scale production. For such application, the performance of ACs depends on the surface area, structure and distribution of pores and electrochemical inertness [1]. These characteristics are directly dependent on the initial carbonaceous precursor and the method of activation to obtain ACs.

The walnut shells are suitable for preparing activated carbon owing to the low moisture content (3–4%), low ash content (1–2%), high density

and easily available precursors [2–4]. Additionally, upon impregnation with less toxic phosphoric acid ($H_3PO_4$) as mild chemical activating agent and high-temperature treatments, carbons with good capacitive performance are produced [5]. However, the correlation between temperature of walnut shell activation in presence of $H_3PO_4$ and the capacitive behavior of resulting ACs has not been yet reported.

Phosphoric acid treatment promotes dehydrogenation and accelerated carbonization occurring at a moderate high temperature treatment (HTT) [6], which may be too low when other reagents such as potassium hydroxide are used. According to [6–7] activation of lignocellulosic biomass impregnated with phosphoric acid carried out in the range of 350–450 °C contributes to the formation of microporous ACs with the highest specific surface area which is in the range of 1500–1900 $m^2$ $g^{-1}$.

---

By use of TG-DTG diagrams studied by different authors it is shown that the pyrolysis of $H_3PO_4$-activated carbonaceous material is delayed compared to the non-$H_3PO_4$ activated materials, wherein the shift of the main decomposition peak usually exceeds 300 °C [8–9]. A progressive narrowing of the pores and loss of accessible surface area resulted from the secondary contraction exerts a dominant effect above 450 °C [7]. Finally, in the range of 580–720 °C the cleavage of previously formed bonds, and their subsequent recombination in the condensed poly-aromatic compounds has been proposed [8]. Nevertheless, recent studies in high temperature treatment of $H_3PO_4$-impregnated graphene aerogels, attempted to bring a new look at the possibility of this method [10–11]. In particular, due to the evolution of elemental phosphorus occurring during activation when the temperature exceeds 800 °C, the additional nanoporosity can be formed.

In this study, a highly efficient method for high-temperature treatment of walnut shells in presence of mild 40 wt.% $H_3PO_4$ is presented. The aim of work is to develop micro- and mesoporous ACs possessing developed specific surface area and a high volume of micropores. Furthermore, these ACs are used as electrode material in SCs to establish the influence of the processing temperature on the electrochemical charge storage.

## 2. Experimental

Cleaned, dried and crushed walnut shells (*Juglans regia*) were derived from local farms of Almaty province, Kazakhstan, and impregnated with 40 wt.% aqueous solution of $H_3PO_4$ with ratio of activator to precursor equal to 3:1. Then resulting mixture was placed in a ceramic crucible and activated for 45 min at 400 °C, 500 °C and 800 °C under nitrogen atmosphere inside a shaft furnace. Carbons obtained at these temperatures are described in manuscript as P-400, P-500 and P-800 respectively. The post-treatment of one sample (activated at 400 °C) was performed at 800 °C, further described in the text as P-400-M. The nitrogen adsorption isotherms were determined with an Autosorb-1 (Quantachrome instruments, UK) in the range of relative pressures from 0.005 to 0.991 realized at -196 °C. BET specific surface area was calculated from the range of relative pressure values below 0.1. The modified model of non-local density functional theory (2D-NLDFT) was used to determine pore volume and pore size distribu-

tion (PSD). The morphology of ACs was investigated by scanning electron microscopy (SEM) using a QUANTA 3D 200i microscope («FEI», USA) with accelerating voltage of 15 kV and the elemental composition by using energy dispersive X-ray analyzer EDAX TEAM (Ametek, USA). Raman spectroscopy was performed with a Raman spectrometer Renishaw InVia Basis (Renishaw plc, UK) using excitation wavelength of 633 nm and exposure time 100 s.

For evaluating electrochemical performance of ACs in SCs, composite electrodes pellets by mixing 90 wt.% of AC, 5 wt.% of polytetrafluoroethylene (PTFE) from Sigma-Aldrich and 5 wt.% of carbon black (C-65, Timcal C-NERGY Imerys). Two-electrode cells were realized in Teflon Swagelok® vessel using 1 mol $L^{-1}$ $Li_2SO_4$ aqueous electrolyte, Whatman GF/A membrane separator and SS 316L current collectors. The cyclic voltammetry (CV), galvanostatic charge/discharge (GCPL) and electrochemical impedance spectroscopy (EIS) in the range 1 mHz to 100 kHz were carried out by using a VMP-3 multichannel potentiostat/galvanostat (BioLogic Instruments, France).

## 3. Results and Discussion

SEM images in Fig. 1(a) present the surface morphology of ACs prepared through activation at temperatures from 400 °C to 800 °C resembling the loose cellular structure and possess highest open work texture represented by interconnected cavities formed owing to organic volatiles evolution. The release of volatiles resulted in reduced oxygen and the mineral part of carbonized material related with potassium leaching which was replaced by phosphorus. However, the mass content of phosphorus is reduced with increasing activation temperature from 500 to 800 °C. In such a case phosphate groups are formed that convert to polyphosphate groups [6–8], and apparently further decompose at higher temperatures; the similar trend was previously discussed in [12–13]. Consequently, the submicron sized channel openings and fissures protruding to the surface are formed which are clearly visible after post treatment in P-400-M.

The Raman spectra of resulting ACs in Fig. 1(b) display almost linear dependence between the intensity of D-band and the temperature of chemical activation. The gradual development of porosity, its reorganization and progressive narrowing of the nanopores might be associated with $I_D/I_G$ ratio.

Indeed, the high D-band intensity and $I_D/I_G$ ratio of 1.09 for P-400-M confirm the development of defects and graphitic disorders. The presence of shoulder peak in the region of 1150 cm$^{-1}$ is referred to the carbon-hydrogen bonds [14–15] which can be reflected from the certain condensed polyaromatic structures formed due to the activation of lignocellulosic biomass by phosphoric acid [7].

The nitrogen adsorption isotherms in Fig. 2(a) present high adsorption capacity of the ACs. Nearly unchanged BET surface area ~ 2000 m$^2$ g$^{-1}$ shows the essential development of porous structure confirmed by changing meso- and micro-pore volumes with increasing activation temperature from 400 to 800 °C (Table 1). This trend is probably caused by cleavage of bonds connecting the biopolymer fragments and subsequent collapse of porosity and burnout of narrow pores leads to merging into larger pores. Additionally, Fig. 2(b) confirms that the pore size distributions from polymodal structure attributed to AC at 400 °C is gradually shifted to bi-modal with increasing of activation temperature. Furthermore, the post-treatment of AC (prepared at 400 °C) performed at 800 °C promotes the reorganization of porosity with a mesopore volume of 0.86 cm$^3$ g$^{-1}$ and average micropore size of 0.88 nm which is appropriate for ionic adsorption. Noticeably, the post-treatment enables highest surface area calculated by 2D-NLDFT (SDFT) confirming the high effective surface utilized in capacitive charging for P-400-M (Table 1).
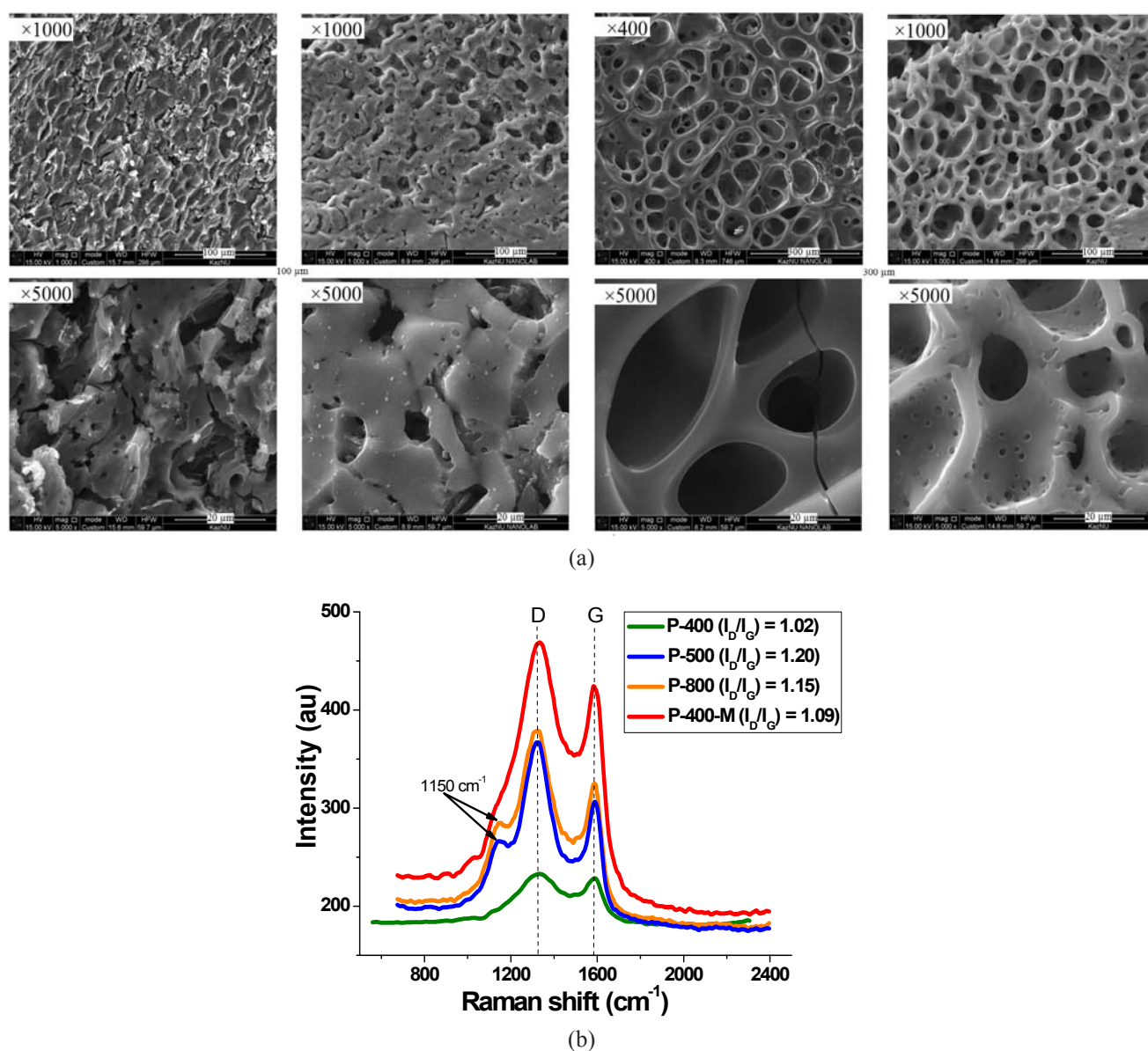


(a)



(b)

Fig. 1. (a) SEM images and (b) Raman spectra of H$_3$PO$_4$-impregnated walnut shell based ACs P-400, P-500, P-800 and P-400-M.
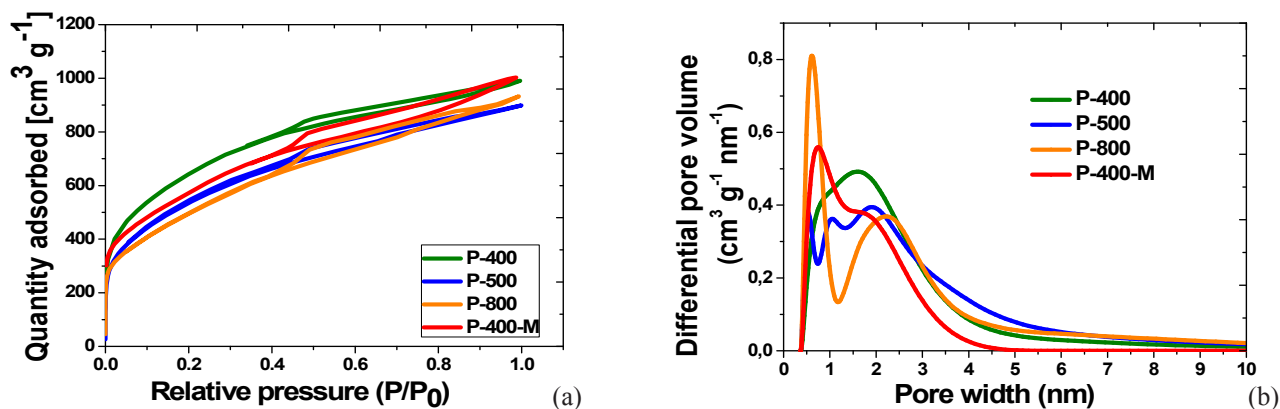
Fig. 2. (a) Nitrogen adsorption/desorption isotherms realized at -196 °C, (b) Pore size distribution (PSD) using the 2D-NLDFT model of $H_3PO_4$-impregnated WS based ACs P-400, P-500, P-800 and P-400-M.

**Table 1**
Textural parameters of ACs prepared from WS by chemical activation with $H_3PO_4$

| # | Material | $S_{BET}$ (m$^2$·g$^{-1}$) | $S_{DFT}$ (m$^2$·g$^{-1}$) | $V_{micro}$ (cm$^3$·g$^{-1}$) | $V_{meso}$ (cm$^3$·g$^{-1}$) | Average micropores size (nm) |
|---|---|---|---|---|---|---|
| 1 | P-400 | 2095 | 1621 | 0.52 | 0.73 | 1.13 |
| 2 | P-500 | 1987 | 1536 | 0.46 | 0.72 | 1.01 |
| 3 | P-800 | 1956 | 1578 | 0.67 | 0.32 | 0.76 |
| 4 | P-400-M | 2055 | 1789 | 0.58 | 0.88 | 0.86 |

**Table 2**
Specific surface area (BET) calculated for WS-based carbons

| # | Precursor | Activator | Specific surface area (BET) | Source |
|---|---|---|---|---|
| 1 | Walnut shell | $CO_2$ | 697 m$^2$·g$^{-1}$ | [16] |
| 2 | Walnut shell | $ZnCl_2$ | 1452 m$^2$·g$^{-1}$ | [17] |
| 3 | Walnut shell | KOH | 2044 m$^2$·g$^{-1}$ | [18] |
| 4 | Walnut shell | $H_3PO_4$ | 2095 m$^2$ g$^{-1}$ | Present work |

The following Table 2 briefly summarizes BET specific surface area typical for carbons based on WS activated by various oxidizing agents, such as zinc chloride, potassium hydroxide or gaseous carbon dioxide. One can see that the value of specific surface area calculated for P-400 is higher than that of all the carbons represented in Table 2.

The CVs and GCPL curves for AC/AC cells with prepared carbons up to 1.0 V in 1 mol L$^{-1}$ Li$_2$SO$_4$ are presented in Fig. 3(a) and (b) respectively. CV for P-400 is characterized by poor capacitive traces and the further rising of activation temperature up to 500 °C does not change much the charging characteristics. Even for the carbon activated at 800 °C, the CV shape is not rectangular suggesting the hindrance to ionic movement inside the porosity. However, implementing P-400-M resulted in quasi-perfect shape of CV. In such a carbon, the porous structure reorganization due to post-treatment facilitates the movement of ions within porosity. Similarly, the rectangular CV and symmetric GCPL for cell using P-400-M shows the absence of faradaic contributions owing to loss of oxygenated functionalities giving rise to highly accessible porosity. Nyquist plots in Fig. 3(c) reveal a shift in charge transfer resistance (R$_{ct}$) from 4.4 (P-400) to 1.6 Ω (P-400-M) and the former demonstrates low ESR (0.4 Ω). However, improved R$_{ct}$ values for P-400-M indicate significant modification in the porous structure leading to facile diffusion of electrolyte. Moreover, the cell using P-400-M demonstrates higher capacitance than cell using DLC Supra 30 (Fig. 3(d)).

Further, AC/AC cell using P-400-M electrodes and 1 mol L$^{-1}$ Li$_2$SO$_4$ polarized up to 1.5 V demonstrates nearly rectangular CVs and symmetric GCPL curves at 0.2 A g$^{-1}$. Furthermore, this cell exhibits a capacitance of 123 F g$^{-1}$ (0.2 A g$^{-1}$) and constant capacitance at 1.0 A.g$^{-1}$ for 5000 galvanostatic charge/discharge showing a good state-of-health during long-term cycling.
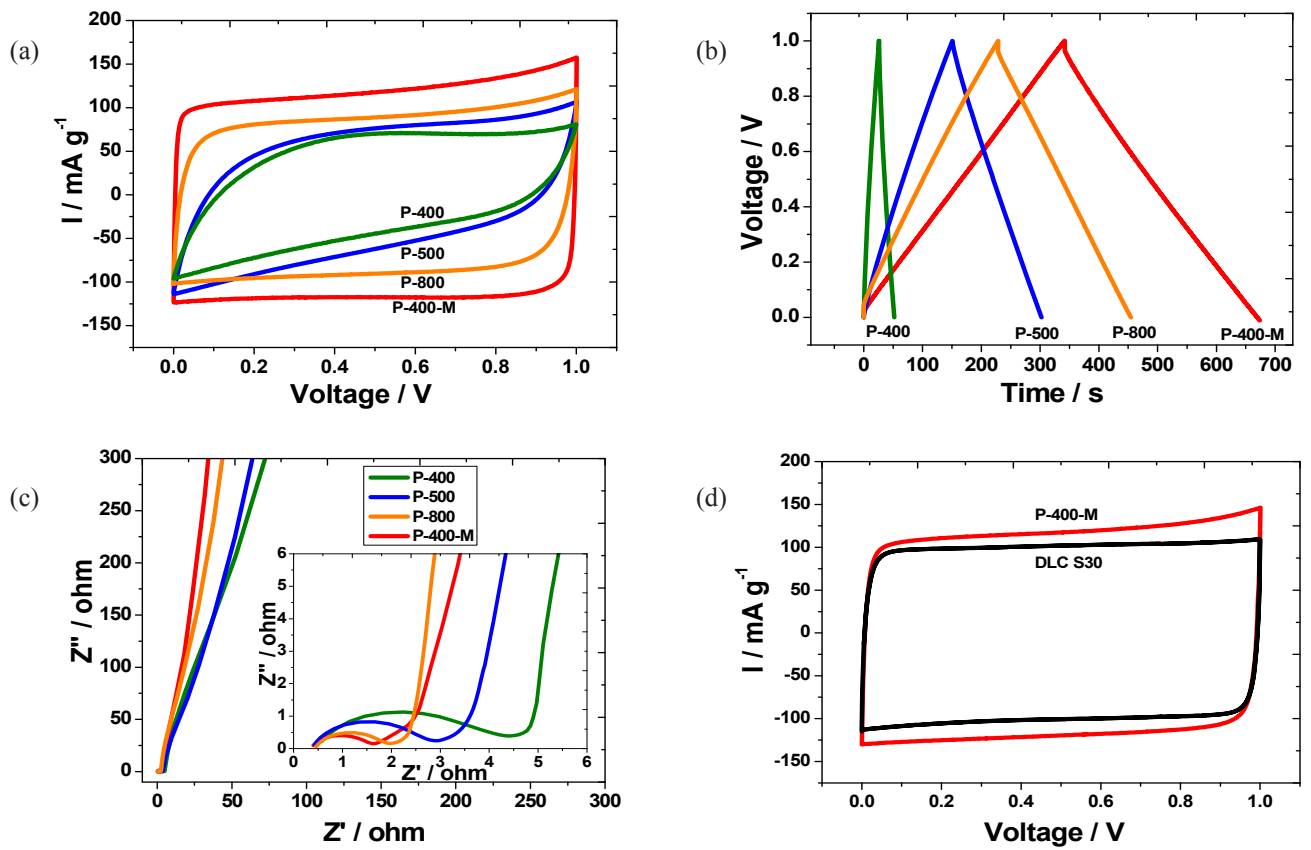
Fig. 3. (a) CVs at 2 mV s$^{-1}$, (b) GCPL curves at 200 mA g$^{-1}$ and (c) Nyquist plot at OCV of two-electrode AC/AC cells in 1 mol L$^{-1}$ Li$_2$SO$_4$ ; (d) CV comparison of AC/AC cells using P-400-M and DLC Supra 30 in 1 mol L$^{-1}$ Li$_2$SO$_4$.
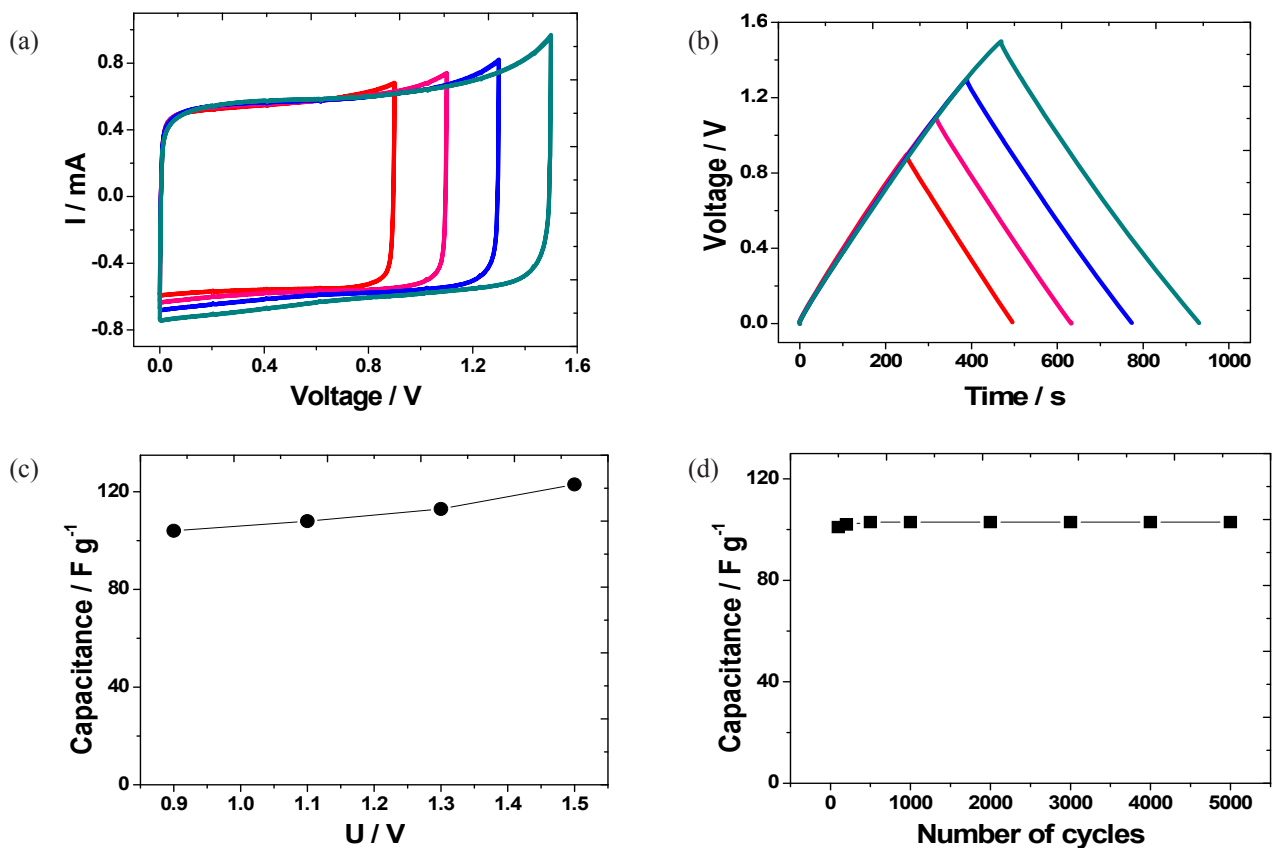


Fig. 4. (a) CVs, (b) GCPL and (c) capacitance vs voltage of AC/AC cells (P-400-M) in 1 mol L$^{-1}$ aqueous Li$_2$SO$_4$ up to 1.5 V (d) Galvanostatic charge-discharge cycling for 5000 cycles up to 1.5 V at 1.0 A g$^{-1}$.

When comparing the capacitance values obtained by DLC Supra 30, one can see the advantage of walnut shell based carbon obtained by mild phosphoric activation exhibiting around 70% capacitance enhancement. Hence, high temperature treatment of walnut shell precursor with mild $H_3PO_4$ results in high surface area carbon perfectly adapted for application as electrode material for realizing electrochemical capacitors in 1 mol·L$^{-1}$ $Li_2SO_4$.

## 4. Conclusions

Carbons produced from the walnut shell activated by $H_3PO_4$ at 400 °C are characterized by highest specific surface area which exceeds 2000 m$^2$·g$^{-1}$. Despite a well-developed porosity this type of carbonaceous materials are not able to be utilized as electrode materials for ECs due to the poor capacitive traces and high electrical resistivity. Increasing of activation temperature up to 800 °C improves electrochemical performance, but CV shape is not rectangular suggesting the hindrance to ionic movement inside the porosity of carbon electrodes. Furthermore the release of elemental phosphorus taking place during pyrolysis at high temperatures limits the practical importance of this method. As an alternative, it is proposed to use the thermal post-treatment of $H_3PO_4$-activated walnut shell at 800 °C which results in high specific surface area of carbon material. This approach makes possible to keep high values of porous texture without its excessive shrinkage and to produce carbon materials perfectly adapted for the charge storage in supercapacitors. This method is highly efficient and also economically feasible, since the post-treated materials are based on carbons produced at low temperatures. Supercapacitors constructed by implementing these carbons in 1 mol·L$^{-1}$ $Li_2SO_4$ exhibit square-shape CVs, symmetric GCPL curves, low resistance and excellent capacitance retention during 5000 galvanostatic charge/discharge cycles at 1.5 V. Such superior electrochemical performance suggests that post-treatment of carbons (after $H_3PO_4$ activation) leads to developed porous texture appropriate for charge storage applications.

## Acknowledgments

## References

[1]. E. Frackowiak, F. Béguin, *Carbon* 39 (2001) 937–950. DOI: 10.1016/S0008-6223(00)00183-4

[2]. J. Yang, K. Qiu, *Chem. Eng. J.* 165 (2010) 209–217. DOI: 10.1016/j.cej.2010.09.019

[3]. W-S. Choi, W-G. Shim, D-W. Ryu, M-J Hwang, H. Moon, *Microp. Mesopor. Mat.* 155 (2012) 274–280. DOI: 10.1016/j.micromeso.2012.01.006

[4]. S. Azat, R. Busquets, V. Pavlenko, A. Kerimkulova, R. Whitby, Z. Mansurov, *Applied Mechanics and Materials* 467 (2014) 49–51. DOI: 10.4028/www.scientific.net/AMM.467.49

[5]. V. Pavlenko, M. Biisenbayev, F. Béguin, Z. Mansurov, Development of active carbons' porous structure derived from biomasses for their application in supercapacitors, Proc. Int. Conf. "Carbon-2015", July 12-17 (2015), Dresden (Germany), p. 150.

[6]. H. Benaddi, T.J. Bandosz, J. Jagiello, J.A. Schwarz, J.N. Rouzaud, D. Legras, F. Béguin, *Carbon* 38 (2000) 669–674. DOI: 10.1016/S0008-6223(99)00134-7

[7]. M. Jagtoyen, F. Derbyshire, *Carbon* 36 (1998) 1085–1097. DOI: 10.1016/S0008-6223(98)00082-7

[8]. B.S. Girgis, A.N.A. El-Hendawy, *Microp. Mesopor. Mat.* 52 (2002) 105–117. DOI: 10.1016/S1387-1811(01)00481-4

[9]. G. Zhu, X. Deng, M Hou, K. Suna, Y. Zhang, P. Li, F. Liang *Fuel Process. Technol.* 144 (2016) 255–261. DOI: 10.1016/j.fuproc.2016.01.007

[10]. X. Sun, P. Cheng, H. Wang, H. Xu, L. Dang, Z. Liu, Z. Lei, *Carbon* 92 (2015) 1–10. DOI: 10.1016/j.carbon.2015.02.052

[11]. V. Thirumal, A. Pandurangan, R. Jayavel, K.S. Venkatesh, N.S. Palani, R. Ragavan, R. Ilangovan, *J. Mater. Sci. Mater. Electron.* 26 (2015) 6319–6328. DOI: 10.1007/s10854-015-3219-5

[12]. A.M. Puziy, O.I. Poddubnaya, A. Martínez-Alonso, A. Castro-Muñiz, F. Suárez-García, J.M.D. Tascón, *Carbon* 45 (2007) 1941–1950. DOI: 10.1016/j.carbon.2007.06.014

[13]. M. Myglovets, O.I. Poddubnaya, O. Sevastyanova, M.E. Lindström, B. Gawdzik, M. Sobiesiak, M.M. Tsyba, V.I. Sapsay, D.O. Klymchuk, A.M. Puziy, *Carbon* 80 (2014) 771–783. DOI: 10.1016/j.carbon.2014.09.032

[14]. S. Leyva-Garcíaa, E. Morallón, D. Cazorla-Amorósa, F. Béguin, D. Lozano-Castelló,

*Carbon* 69 (2014) 401–408. DOI: 10.1016/j. carbon.2013.12.042

[15]. H. Kuzmany, R. Pfeiffer, N. Salk, B. Günther, *Carbon* 42 (2004) 911–917. DOI: 10.1016/j. carbon.2003.12.045

[16]. P. Nowicki, R. Pietrzak, H. Wachowska, *Catal. Today* 150 (2010) 107–114. DOI: 10.1016/j. cattod.2009.11.009

[17]. Nazari, H. Abolghasemi, M. Esmaieli, E. Pouyaet, *Appl. Surf. Sci.* 375 (2016) 144–153. DOI: 10.1016/j.apsusc.2016.03.096

[18]. W.-S. Choi, W.-G. Shim, D.-W. Ryu, M.-J. Hwang, H. Moon, *Micropor. Mesopor. Mat.* 155 (2012) 274–280. DOI: 10.1016/j. micromeso.2012.01.006